CEE 598 – Generalized Finite Element Method: Fall 2018 Project 3

Bhavesh Shrimali

Department of Civil and Environmental Engineering, University of Illinois at Urbana-Champaign, IL 61801, USA

Abstract

GFEM with global-local enrichments (GFEM^{gl}) for problems with multiscale structural features is studied. The h-version of GFEM^{gl} is studied for a representative 1-D boundary value problem (BVP) in linear elastostatics with mixed boundary conditions (BCs) in the presence (and absence) of body force (forcing function). GFEM^{gl} can be implemented either as an iterative strategy or as proposed in [5] using a *buffer-zone*. The results when confronted to standard FEM, help to demonstrate the performance of GFEM^{gl} in capturing the multiscale features for non-conforming meshes. The correction of the blending element errors in GFEM^{gl} is attempted through the use of (a): the Stabilized GFEM (SGFEM) [1] with global-local enrichment functions (SGFEM^{gl}) and (b): smoothing the numerical global-local enrichments (SGFEM$^{gl}_{corr}$), along the same line as previously proposed strategies in context of level set functions [3]. Additionally, FEM with higher order PoU (with both Lagrange and $p-$Hierarchical basis) is also used in an attempt to capture the multiscale features for non-conforming FE meshes.

Keywords: Global-Local, Multiscale, Finite Element

1. Introduction

GFEM^{gl} is often used to solve problems with multi-scale features in solid mechanics [5] . Many problems of engineering relevance, in particular those dealing with composite materials behave like the model problem studied below. Homogenized material properties can be used everywhere except at some critical locations near stress risers, cracks, etc. In those regions, the actual material properties must be used for accurate results. However, this may require extremely fine meshes. For such classes of problems GFEM^{gl} provides an effective tool to generate efficient numerical solutions. In general the idea can be extended to any PDE on a bounded domain ($\Omega \subset \mathbb{R}^N$) possibly containing sub-domains exhibiting fine-scale features ($\Omega_m \subseteq \Omega$). Here for definiteness, and in order to aid exposition, consider a 1-D BVP

$$-\frac{\mathrm{d}}{\mathrm{d}x}\left(E(x)A\frac{\mathrm{d}u}{\mathrm{d}x}\right) = T(x), \qquad 0 < x < L \tag{1}$$

with the following choice of mixed boundary conditions

$$u(0) = 0, \quad \text{and} \quad E(L)A\frac{\mathrm{d}u}{\mathrm{d}x}(L) = P \quad \text{with} \quad L = 1 \text{ and } A = 1. \tag{2}$$

An equivalent representation of eq. (1) that readily provides a measure of the total error in a numerical approximation (FEM,GFEM etc.) to the exact solution is given by the following variational principle

$$\min_{u\in\mathcal{V}} \Pi(u) \doteq \left\{\frac{1}{2}\int_0^L E(x)A\left(\frac{\mathrm{d}u}{\mathrm{d}x}\right)^2 dx - \int_0^L T(x)u(x)dx - Pu(L)\right\}. \tag{3}$$

Email address: bshrima2@illinois.edu (Bhavesh Shrimali)

The energy ($\mathcal{U}_h$) correpsonding to a finite element approximation $u_h(x) \in \mathcal{V}_h$ of the exact solution $u(x)$, the energy norm ($\|\cdot\|_{\mathcal{E}}$), and the consequent relative error in the energy norm ($\|\mathbf{e}_h\|_{\mathcal{E}}$), can be given as follows

$$\begin{aligned} \mathcal{U}_h &\doteq \frac{1}{2}\int_0^L E(x)A\left(\frac{\mathrm{d}u^h}{\mathrm{d}x}\right)^2 dx, \quad \|e^h\|_{\mathcal{E}} \doteq \frac{1}{2}\int_0^L E(x)A\left(\frac{\mathrm{d}e^h}{\mathrm{d}x}\right)^2 dx \\ \mathcal{U}_h &\doteq \frac{1}{2}\left(\mathbf{u}^T K \mathbf{u}\right) \quad \text{where} \quad \mathbf{u} = \text{ dofs}, \quad \|\mathbf{e}^h\|_{\mathcal{E}} \doteq \sqrt{\left|\frac{\mathcal{U}(u) - \mathcal{U}_h(u^h)}{\mathcal{U}(u)}\right|}. \end{aligned} \tag{4}$$

For the problem at hand, the Young's modulus, $E\,(x)$ is given by

$$E(x) = \begin{cases} E_H & \text{if } \ 0 \le x \le 3L/8 \\ \widetilde{E}(x) & \text{if } \ 3L/8 < x < 5L/8 \\ E_H & \text{if } \ 5L/8 \le x \le L, \end{cases} \tag{5}$$

where the homogenized modulus E_H is given in terms of the volume fractions (ν_1 and ν_2) and the Young's modulii (E_1 and E_2) of the constituent materials by

$$E_H = \frac{E_1 E_2}{\nu_1 E_2 + \nu_2 E_1} \quad \text{such that} \quad \nu_1 + \nu_2 = 1 \tag{6}$$

The oscillatory function $\widetilde{E}\,(x)$ describes the variation in the modulus of the composite towards the middle of the domain $\Omega_m = (3L/8, 5L/8)$. The local domain is taken to be $\Omega_{loc} = \left(\frac{L}{4}, \frac{3L}{4}\right)$ (see e.g. fig. 1),

$$\widetilde{E}\,(x) = \begin{cases} E_1 & \text{if } \ x \in \Omega_1 \\ E_2 & \text{if } \ x \in \Omega_2 \end{cases} \quad \text{where} \quad |\Omega_1| = |\Omega_2| = \Delta L = L/128. \tag{7}$$

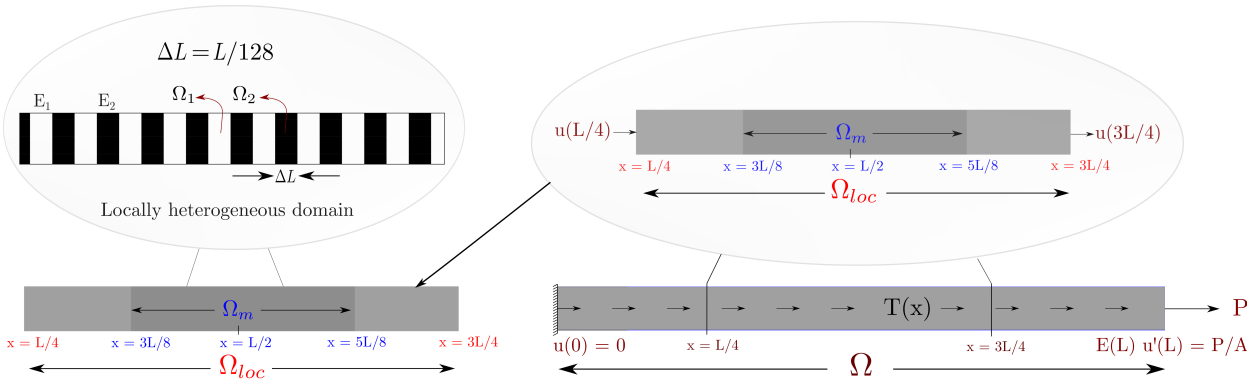

Figure 1: Representative problem domain and boundary conditions for the local domain Ω_{loc}

In context of linear elastostatics, it is assumed that the classical homogenization theory is valid away from the middle of the domain. The solution of the problem in the region where $E\,(x) = \widetilde{E}\,(x)$ varies rapidly due to changes in material property. Hence classical FEM is expected to encounter difficulties in rendering sufficiently accurate results unless a very fine mesh, with the mesh size of the order of the length-scale of the heterogeneity ($\sim \Delta L$) is used. Apriori knowledge of analytical enrichment functions that could render accurate results is often not possible, hence it proves useful to use numerical enrichment functions in such cases.

As with any FE discretization, we consider a partition of the entire domain Ω intro $\mathcal{N}$ non-overlapping domains (uniform element size $= H$) and a locally compact basis $\varphi_\alpha\,(x)$ along with enrichments $E_\alpha\,(x)$. The

main motivation behind GFEM^{gl}, and by the same token SGFEM^{gl} and SGFEM$^{gl}_{corr}$, is to solve the problem using a FE discretization, then consider a local domain Ω_{loc} (along with a *buffer-zone*) with appropriate Dirichlet BCs obtained from the FE solution $u^0_G(x)$. The local problem on Ω_{loc} (with a possibly different element size h) is solved using a FE discretization and the corresponding local solution $u_L(x)$ is used to enrich the region with heterogeneous material properties (in this case Ω_m) and thereby enrich the approximation space of the global solution $u_G(x)$. The enriched global problem in principle can be again used to determine BCs for the local problem and this process can be iteratively continued till a target accuracy has been achieved. For this project only a single pass of the enrichment strategy described above is performed and the corresponding results are presented in section 2 and section 3

2. Boundary Value Problem 1

For this problem GFEM^{gl} (along with SGFEM^{gl} and SGFEM$^{gl}_{corr}$) is studied in absence of any body force i.e. $T(x) = 0$. The following sets of global and local meshes are considered for both FEM and GFEM^{gl} calculations

$$\mathcal{N} = \{8, 16, 32, 64, 128, 256\}\,, \quad \mathcal{N}_{loc} = \{32, 64, 128\}$$

Note that the finest mesh with $\mathcal{N} = 128$ elements exactly conforms to length scale of the heterogeneity (ΔL) and since there is no body force, FEM for this problem is expected to recover the exact solution (up-to discretization error).

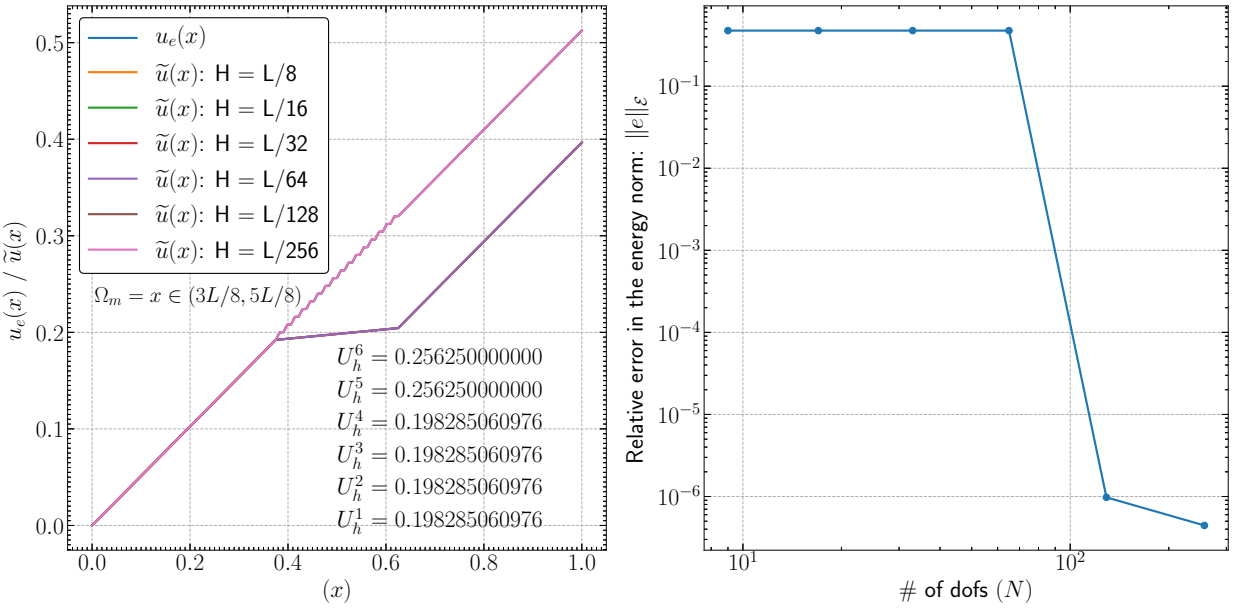

(a) Exact ($u_e(x)$) and FE ($\widetilde{u}(x)$)

(b) Error-vs-# of dofs

Figure 2: FE Solution and Error-convergence for eq. (1) without $T(x)$

This is indeed the case in the figure above. U^i_h refers to the strain energy obtained from the FE solution with the number of elements given by $\mathcal{N}\,(i)$ $(1 \leq i \leq 6)$, and $\widetilde{u}(x)$ refers to the corresponding FE solution. Since the eq. (1) with $T(x) = 0$ admits an exact solution, the corresponding strain energy can be exactly determined

$$\mathcal{U} \equiv U_{ex} = \frac{1}{2}\int_0^1 E(x)\left(\frac{\mathrm{d}u}{\mathrm{d}x}\right)^2 dx = \frac{41}{160} = 0.256250000000 \tag{8}$$

The enrichment functions for GFEM^{gl}, SGFEM^{gl}, SGFEM$^{gl}_{corr}$ are given as follows:

- GFEM^{gl} The local solution $u_L(x)$ is used as an enrichment function for the global problem.

$$E_\alpha(x) = u_L(x)$$

- SGFEM^{gl}: The FE interpolant of the local solution $\mathcal{I}_{\omega_\alpha}(u_L(x))$ is subtracted from the local solution $u_L(x)$ and the resulting function is used as the enrichment function.

$$\widetilde{E}_\alpha(x) = u_L(x) - \mathcal{I}_{\omega_\alpha}(u_L(x))$$

- SGFEM$^{gl}_{corr}$: The smoothed local solution is used as an enrichment for the global problem.

$$\widehat{E}_\alpha(x) = \begin{cases} u_L(3L/8) & \text{if} \quad x < 3L/8 \\ u_L(x) & \text{if} \quad 3L/8 <= x <= 5L/8 \\ u_L(5L/8) & \text{if} \quad 5L/8 < x \end{cases}$$

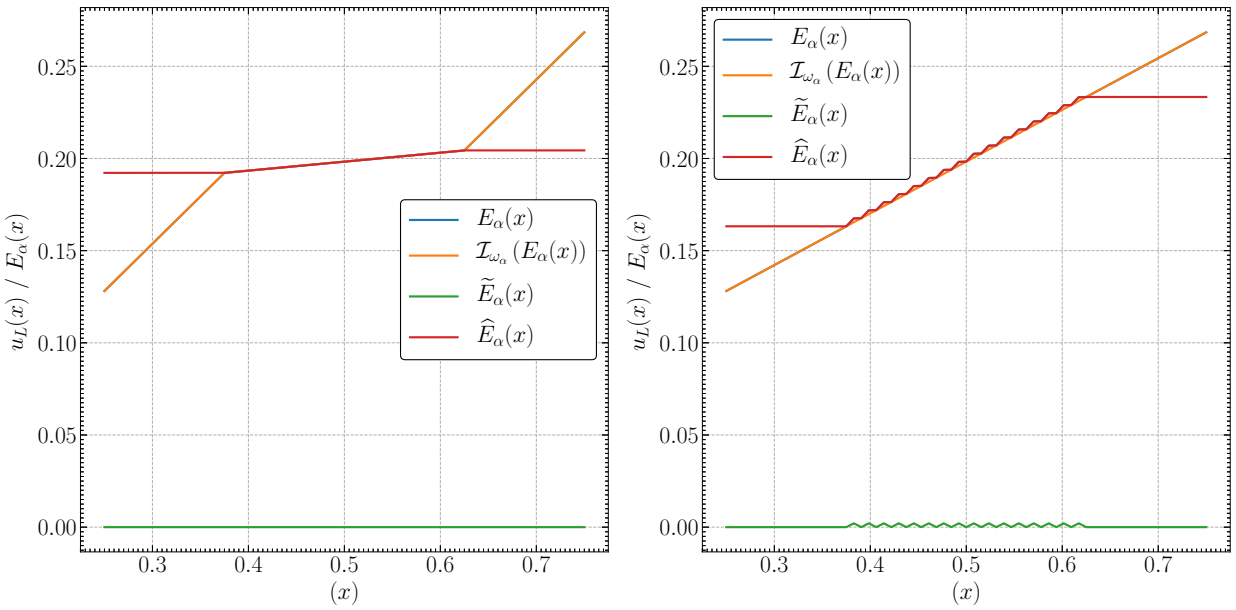

(a) $h = L/64$ (b) $h = L/128$

Figure 3: BVP1: Enrichment functions for $h = \{L/64,\ L/128\}$

The oscillatory behavior introduced by the Young's modulus eq. (7) can be accurately captured by the enrichment functions only for a conforming local mesh (see fig. 3 above). For non-conforming local meshes, the numerical enrichment function isn't accurate and hence does not enrich the global solution well enough (see fig. 9a below).

Note. : The enrichment function, in fig. 3b and its derivative fig. 4b for SGFEM^{gl} are zero (up-to machine precision) in the blending elements, whereas for SGFEM$^{gl}_{corr}$ they are constant. This is reflected in the significantly lower values of the relative errors for these enrichments for a conforming local mesh $h = L/128$. However when using SGFEM^{gl} to perform calculations with a conforming global mesh ($H <= L/128$) when both the enrichment and its derivative become zero in reproducing elements as well, thereby rendering an

indefinite linear system, FP errors, in particular the discretization errors, must be eliminated to get an accurate solution. A conforming global mesh for this problem should recover the FE solution, i.e. the dofs corresponding to the enrichment functions should be equal to zero. One *ad-hoc* strategy is to set the elements in the principal diagonal of the global stiffness matrix to **1** (or any finite value)[2]. This prevents round-off errors when solving the linear system through Gaussian elimination, or other direct methods. It is worth mentioning that similar problems do not arise with Krylov subspace methods capable of handling indefinite linear systems such as `minres`, `gmres` etc. However the convergence of these methods is often slow without a good estimate for the preconditioner. In such cases, Multigrid methods can provide with a sufficiently accurate preconditioner [7], at least for the type of problem studied here.

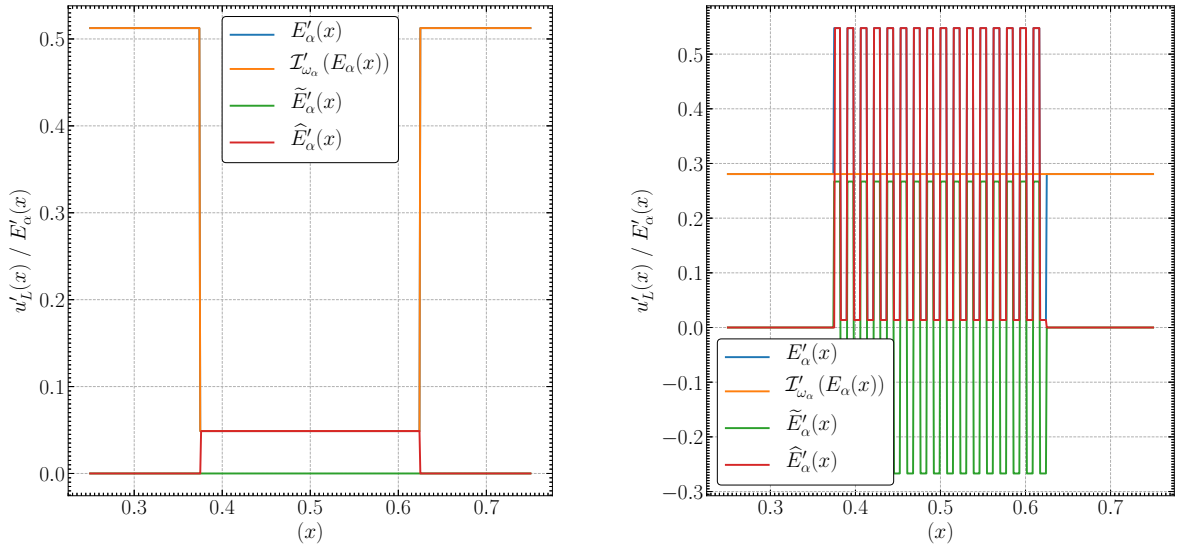

(a) $h = L/64$ (b) $h = L/128$

Figure 4: BVP1: Derivatives of the enrichment functions for $h = \{L/64,\ L/128\}$

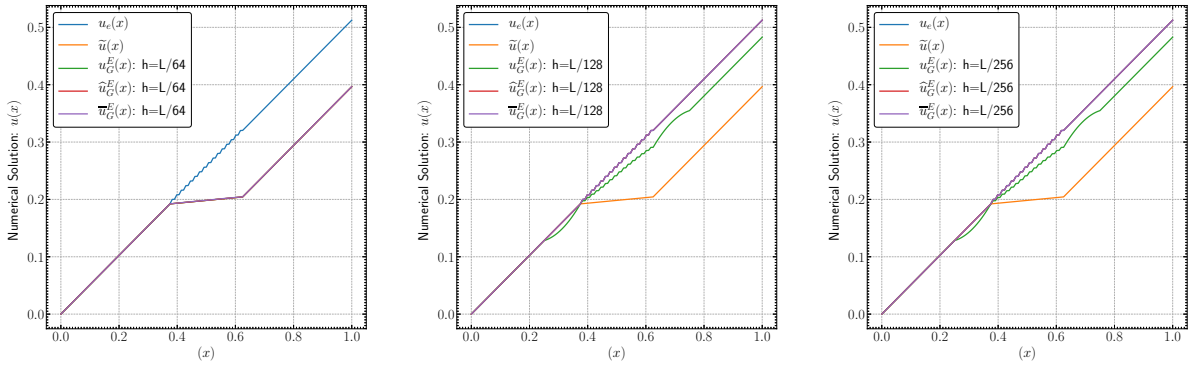

(a) $h = L/64$ (b) $h = L/128$ (c) $h = L/256$

Figure 5: FEM and GFEM solutions with $\mathcal{N} = 8$ elements for (a)$h = L/64$, (b)$h = L/128$ and (c)$h = L/256$. u_G^E, $\widehat{u}_G^E$ and $\overline{u}_G^E$ denote the GFEM^{gl}, SGFEM^{gl}, and SGFEM$^{gl}_{corr}$solutions respectively.

The corresponding plots containing the numerical solutions (for FE,GFEM^{gl}, SGFEM^{gl}, SGFEM$^{gl}_{corr}$) along with the exact solution for for $\mathcal{N} = \{16, 32, 64, 128\}$ elements are given below

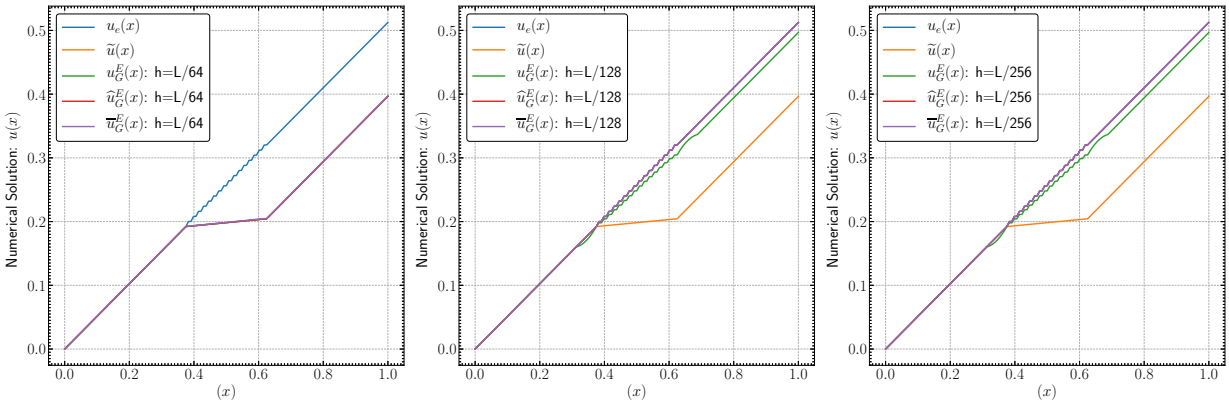

(a) $h = L/64$ (b) $h = L/128$ (c) $h = L/256$

Figure 6: FEM and GFEM solutions with $\mathcal{N} = 16$ elements with (a) $h = L/64$, (b) $h = L/128$ and (c) $h = L/256$

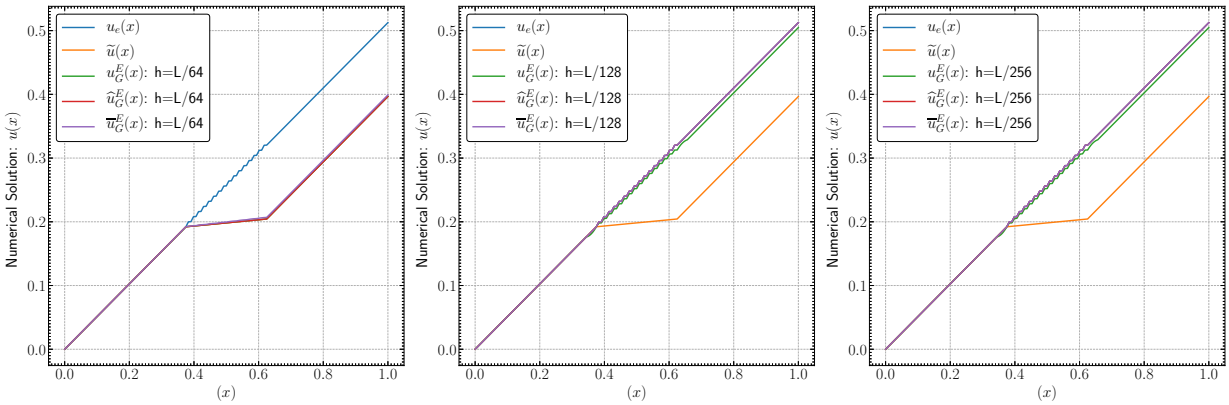

(a) $h = L/64$ (b) $h = L/128$ (c) $h = L/256$

Figure 7: FEM and GFEM solutions with $\mathcal{N} = 32$ elements with (a) $h = L/64$, (b) $h = L/128$ and (c) $h = L/256$

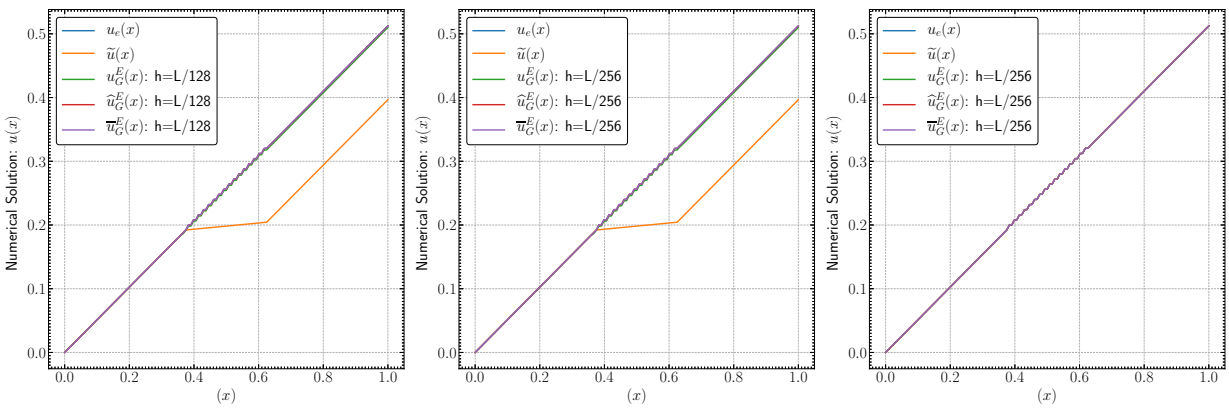

(a) $h = L/128$ (b) $h = L/256$ (c) $h = L/256$

Figure 8: FEM and GFEM solutions with $\mathcal{N} = 64$ elements with (a) $h = L/128$, (b) $h = L/256$ and $\mathcal{N} = 128$ elements with (c) $h = L/256$

GFEM^{gl} leads to smaller errors in the blending elements for non-conforming global meshes ($\mathcal{N} = 8, 16, 32, 64$) and conforming local meshes ($h <= L/128$). For a conforming global mesh, it recovers the exact solution up-to numerical round-off. On the other hand in this case **by design both SGFEM^{gl} and SGFEM$^{gl}_{corr}$ eliminate the approximation error in the blending elements**, thereby enriching the trial space ($\mathcal{V}_h$) such the numerical solution can accurately represent the jump in the gradient values as well as maintain C^0 continuity characteristic of the exact solution. This is verified below in fig. 9b and fig. 9c. The scaled condition numbers in fig. 9d-9e indeed verify that the conditioning of SGFEM^{gl} is no worse than FEM [1]. These results are summarized in table 1

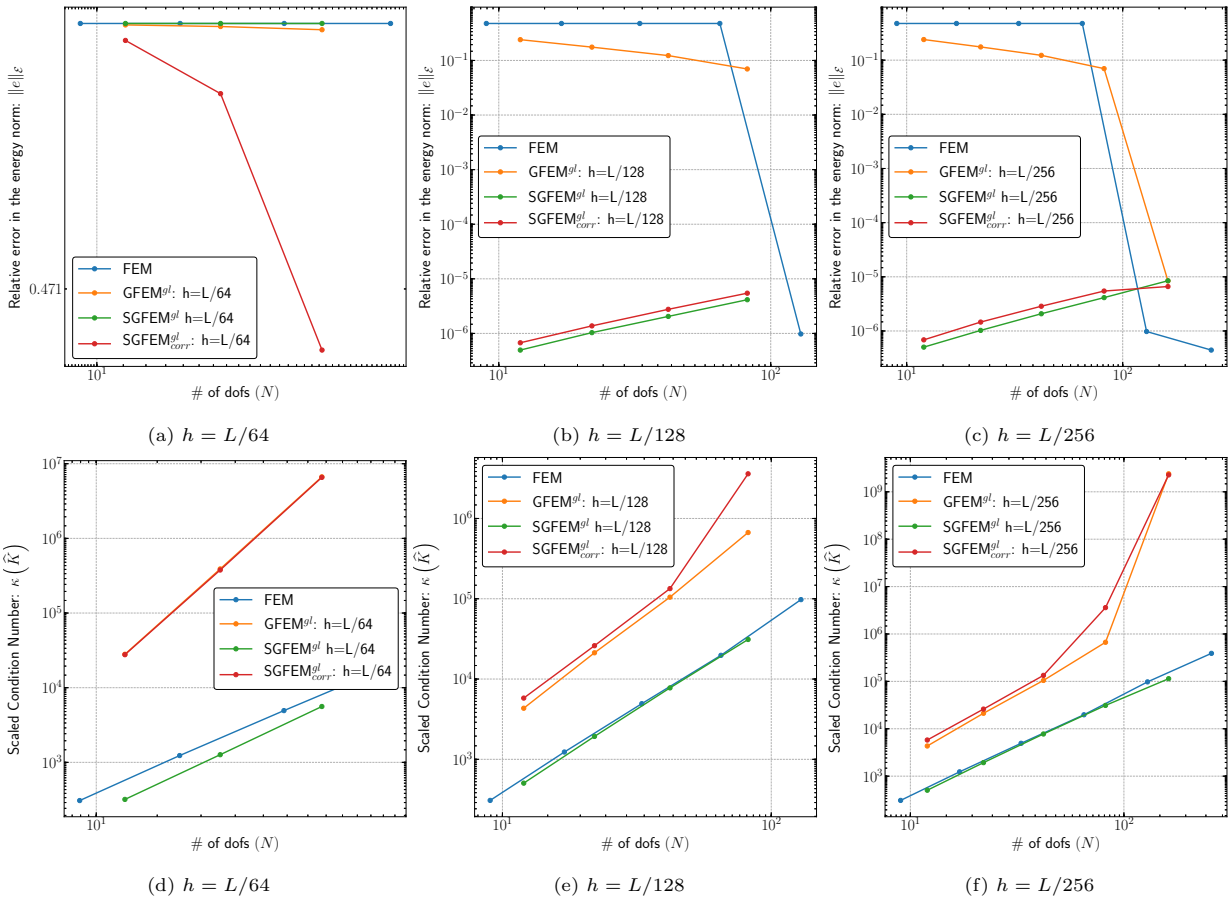

(a) $h = L/64$ (b) $h = L/128$ (c) $h = L/256$

(d) $h = L/64$ (e) $h = L/128$ (f) $h = L/256$

Figure 9: Relative error $\|e\|_\mathcal{E}$ and Scaled condition number $\kappa\left(\widehat{K}\right)$ vs No. of dofs (N) for (a)$h = L/64$, (b)$h = L/128$ and (c)$h = L/256$

To summarize, the following remarks in order :

- FEM (more precisely h-version FEM with $p = 1$) with non-conforming (global) meshes does not converge at all. Piecewise linear polynomials cannot approximate the material interface within an element and consequently the jumpy in the gradient of the solution. This is a 1D example of a classical material interface problem [6].
- In case of GFEM^{gl} a conforming mesh with $h <= L/128$ or equivalently $\mathcal{N}_{loc} = \{64, 128\}$ for the local problem (in Ω_{loc}) is required to accurately capture the material inhomogeneity. The resulting enriched global solution accurately approximates the exact solution in the reproducing elements but suffers from errors in the blending elements.

- Both SGFEM^{gl}, and SGFEM$^{gl}_{corr}$improve upon this shortcoming of GFEM^{gl}, and (by design) eliminate the blending element errors yet maintaining the accuracy in the reproducing elements, with SGFEM^{gl} bringing an added advantage of improved conditioning of the linear system. **Note that the superior performance of SGFEM^{gl} in this case is an exception since, in general it only serves to improve the conditioning of the linear system**. SGFEM^{gl} by definition makes the enrichment zero only at the nodes of the element. But since the local solution itself is linear over the blending elements, its finite element interpolant ($\mathcal{I}_{\omega_\alpha}$) is also linear, and hence the enrichment function $\widetilde{E}_\alpha(x)$ is identically zero over the entire blending element.

Method	**L/H**	**L/h**	$\|e\|_{\mathcal{E}}$	$\kappa\left(\widehat{K}\right)$
GFEM^{gl}	8	64	0.475587	2.80E+04
		128	0.240187	4.33E+03
		256	0.240187	4.33E+03
	16	64	0.475587	3.90E+05
		128	0.175371	2.12E+04
		256	0.175371	2.12E+04
	32	64	0.475587	6.67E+06
		128	0.122739	1.05E+05
		256	0.122739	1.05E+05
	64	128	0.0697982	6.68E+05
		256	0.0697982	6.68E+05
	128	256	8.41E-06	2.40E+09

(a) GFEM^{gl} – Relative Error and Scaled Condition Number

Method	**L/H**	**L/h**	$\|e\|_{\mathcal{E}}$	$\kappa\left(\widehat{K}\right)$
SGFEM^{gl}	8	64	0.47561	3.19E+02
		128	4.95E-07	5.05E+02
		256	5.03E-07	5.05E+02
	16	64	0.47561	1.27E+03
		128	1.03E-06	1.93E+03
		256	1.02E-06	1.93E+03
	32	64	0.47561	5.60E+03
		128	2.05E-06	7.76E+03
		256	2.08E-06	7.76E+03
	64	128	4.14E-06	3.11E+04
		256	4.13E-06	6.68E+05
	128	256	8.45E-06	1.14E+05

(b) SGFEM^{gl} – Relative Error and Scaled Condition Number

Method	**L/H**	**L/h**	$\|e\|_{\mathcal{E}}$	$\kappa\left(\widehat{K}\right)$
SGFEM$^{gl}_{corr}$	8	64	0.475342	2.77E+04
		128	6.74E-07	5.79E+03
		256	0.240187	5.79E+03
	16	64	0.4745	3.77E+05
		128	1.37E-06	2.60E+04
		256	0.175371	2.60E+04
	32	64	0.470471	6.57E+06
		128	2.76E-06	1.34E+05
		256	0.122739	1.34E+05
	64	128	5.46E-06	3.60E+06
		256	5.46E-06	3.60E+06
	128	256	6.61E-06	2.27E+09

(c) SGFEM$^{gl}_{corr}$ – Relative Error and Scaled Condition Number

Method	**L/H**	**L/h**	$\|e\|_{\mathcal{E}}$	$\kappa\left(\widehat{K}\right)$
FEM	8		0.47561	307.823
	16		0.47561	1233.29
	32		0.47561	4935.17
	64		0.47561	19742.7
	128		9.77E-07	97560.8
	256		4.44E-07	390245

(d) FEM– Relative Error and Scaled Condition Number

Table 1: BVP1: Summary of the performance of difference enrichment strategies

Both GFEM^{gl}, and SGFEM$^{gl}_{corr}$ have worse conditioning than standard FEM and SGFEM^{gl}. At the close

of this section it is fitting to highlight that the total approximation space of the FEM (PoU) is accurate enough and hence higher order basis functions are not needed in principle.

3. Boundary Value Problem 2

For this problem the body force $T(x)$ is nonzero and is give by eq. (9) below.

$$T(x) = \frac{2a}{1 + a^2(x - x_b)^2} + \frac{2(1-x)a^3}{\left(1 + a^2(x - x_b)^2\right)^2}(x - x_b), \quad \text{with} \quad a = 30,\ x_b = 0.5 \tag{9}$$

Proceeing along the same lines as in section 2, the same set of global and local meshes are considered here. Since the exact strain energy for this problem cannot be determined analytically, a very fine mesh corresponding to $\mathcal{N} = 1024$ and $\mathcal{N}_{loc} =$ elements (or equivalently $H = L/1024$ and $h = L/2048$) was considered to render a nearly exact strain energy. This is indeed the case, as was verified by doing calculations with higher order FE (with p-order as high as 9 and $\mathcal{N} = 1024$) calculations in section 4. The corresponding enrichment functions fig. 10, and their derivatives fig. 11 are given below.

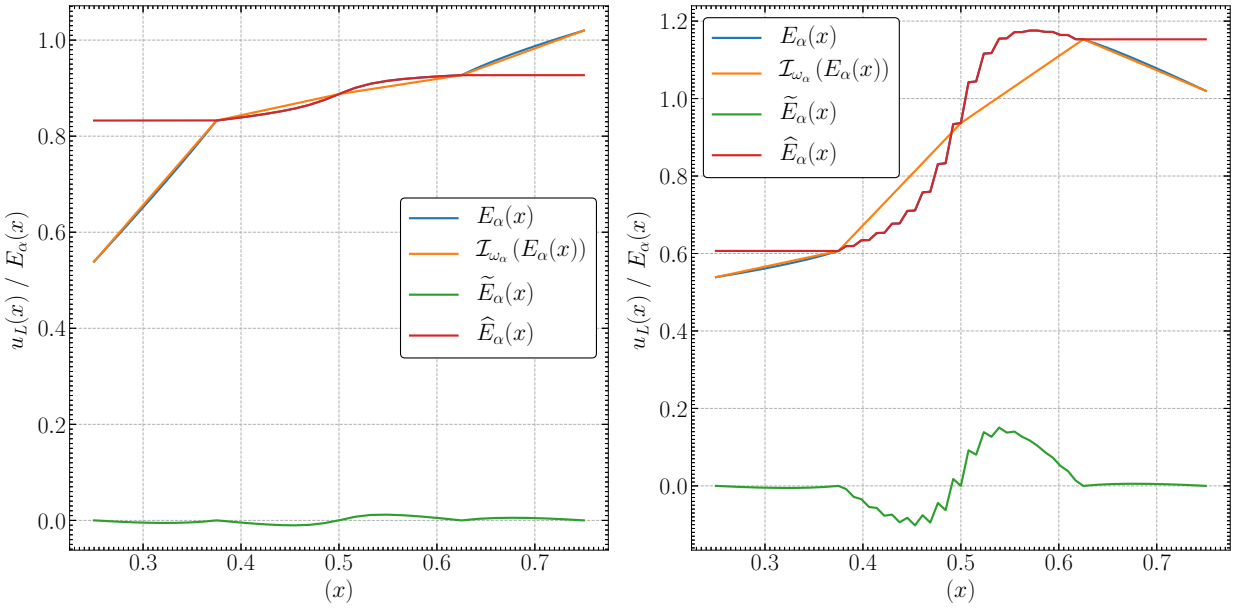

(a) $h = L/64$ (b) $h = L/128$

Figure 10: BVP2: Enrichment functions for $h = \{L/64,\ L/128\}$

The enrichment functions here differ from those in fig. 3 in two aspects:

- The enrichment functions in SGFEM^{gl} are zero only at the nodes of the global mesh and not over the entire blending element. This is expected since the numerical solution is not linear over the entire blending element, but piecewise linear over each local element inside the blending element.
- The derivative of the local solution, and therefore the enrichment function for GFEM^{gl} , and by the same token for SGFEM^{gl}, is no longer zero over the region in the blending elements. Hence the corresponding error over the blending elements is nonzero for both GFEM^{gl}, and SGFEM^{gl} (see fig. 12, fig. 13, fig. 14 and fig. 15 below). However it is indeed zero for SGFEM$^{gl}_{corr}$ since the enrichment function is constant over the blending elements. Mathematically this is also due to the nature of eq. (1)

and the variation of the Young's Modulus eq. (7) (it is still piecewise constant over Ω_1 and Ω_2). This leads to the absence of any dissipative terms like $C(x) \cdot u'(x)$ in eq. (1) which in turn leads to zero blending element error.

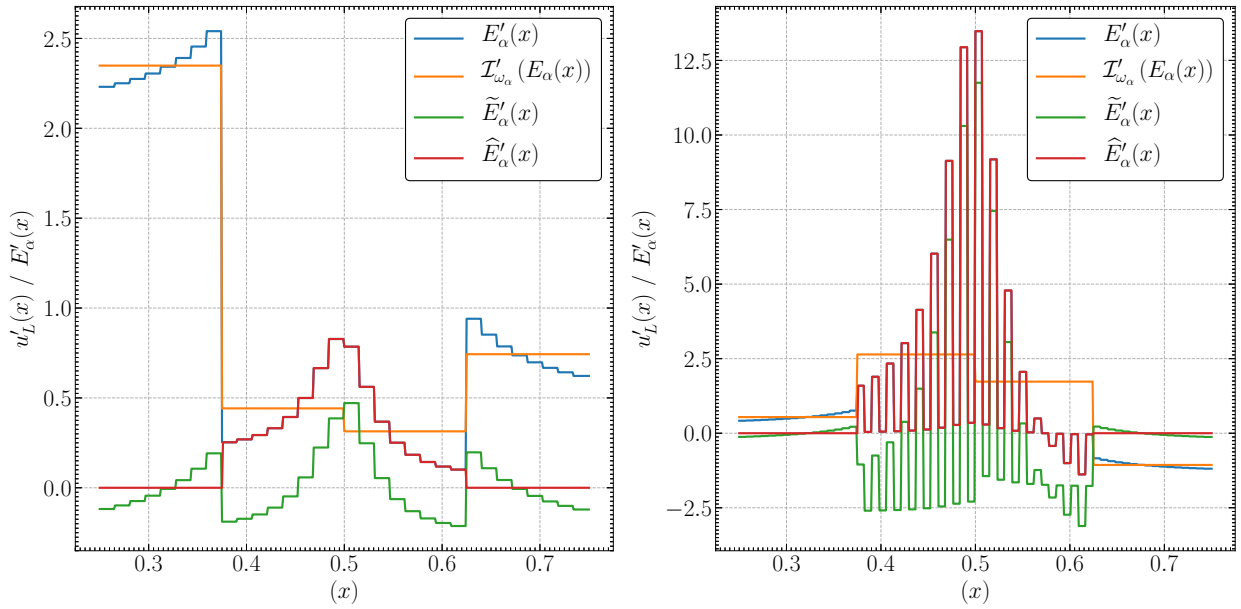

(a) $h = L/64$ (b) $h = L/128$

Figure 11: BVP2: Derivatives of the Enrichment functions for $h = \{L/64,\ L/128\}$

GFEM^{gl} converges slowly due to blending element error and the approximation order of the PoU. Since the exact solution over the domain is highly non-trivial, linear PoU will not be able to approximate the exact solution accurately as in section 2. However for SGFEM$^{gl}_{corr}$ there are no blending element errors, and the convergence is slow due to the PoU itself. This in principle calls for using higher order PoU which is discussed partly in section 4. The numerical solutions for different enrichment strategies for BVP2 are plotted below.

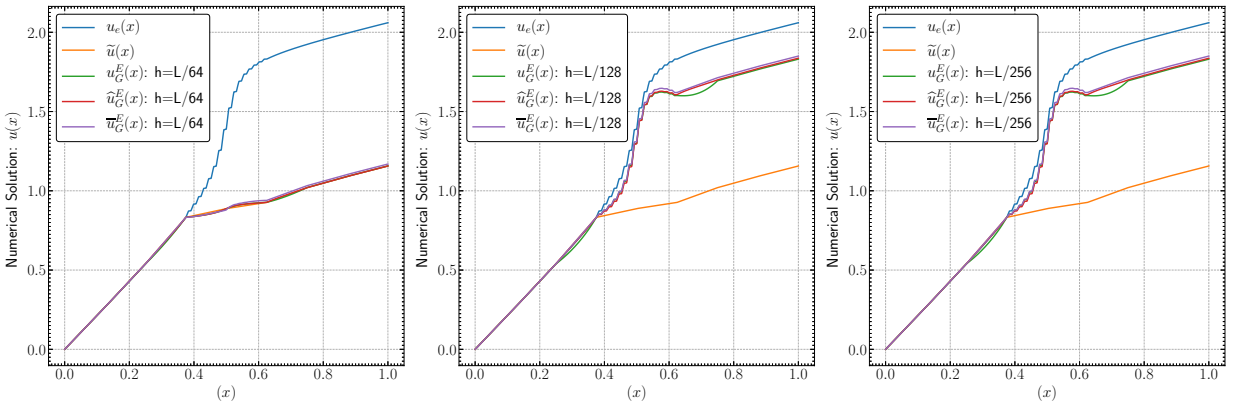

(a) $h = L/64$ (b) $h = L/128$ (c) $h = L/256$

Figure 12: FEM and GFEM solutions with $\mathcal{N} = 8$ elements for (a) $h = L/64$, (b) $h = L/128$ and (c) $h = L/256$

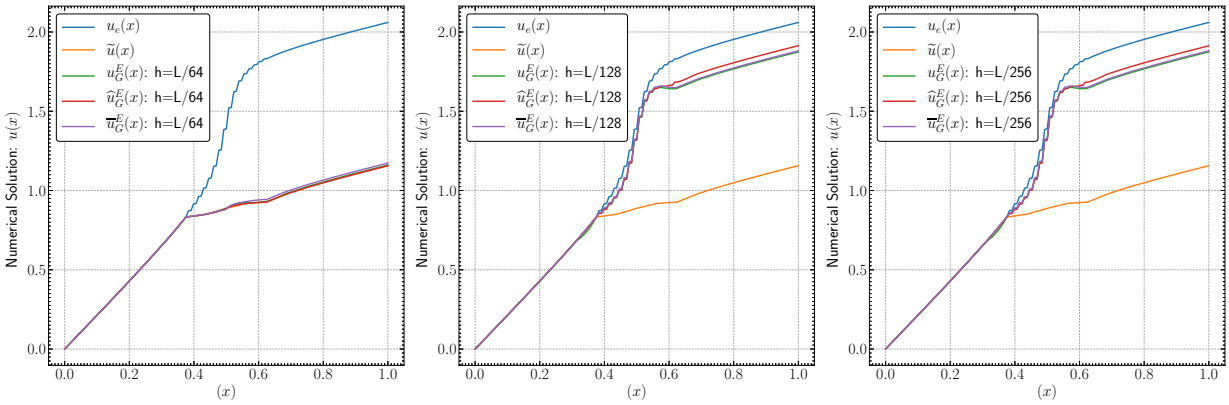

(a) $h = L/64$ (b) $h = L/128$ (c) $h = L/256$

Figure 13: FEM and GFEM solutions with $\mathcal{N} = 16$ elements for (a) $h = L/64$, (b) $h = L/128$ and (c) $h = L/256$

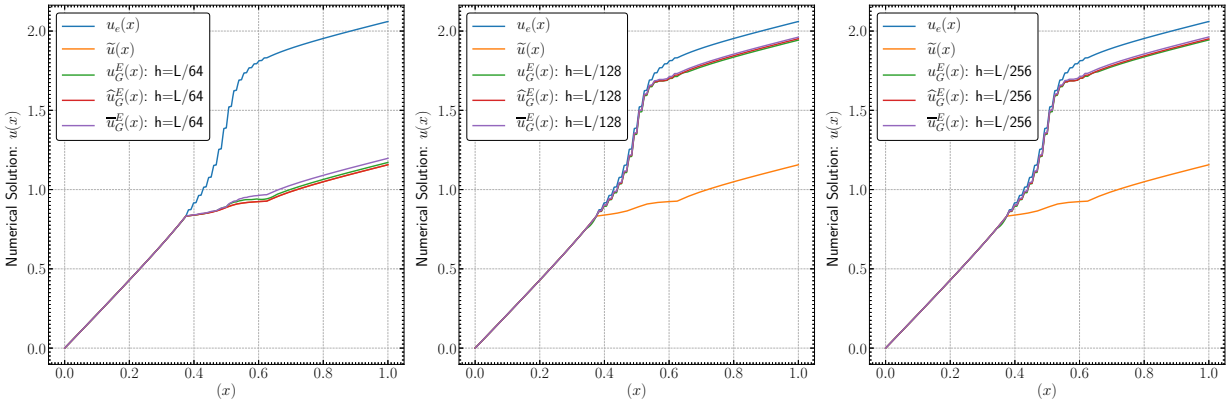

(a) $h = L/64$ (b) $h = L/128$ (c) $h = L/256$

Figure 14: FEM and GFEM solutions with $\mathcal{N} = 32$ elements for (a) $h = L/64$, (b) $h = L/128$ and (c) $h = L/256$

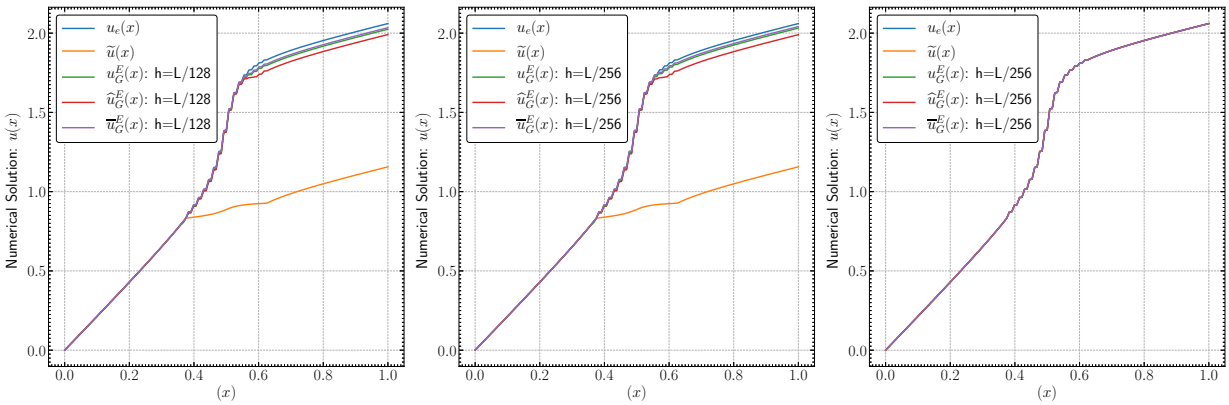

(a) $h = L/128$ (b) $h = L/256$ (c) $h = L/256$

Figure 15: FEM and GFEM solutions with $\mathcal{N} = 64$ elements with (a) $h = L/128$, (b) $h = L/256$ and $\mathcal{N} = 128$ elements with (c) $h = L/256$

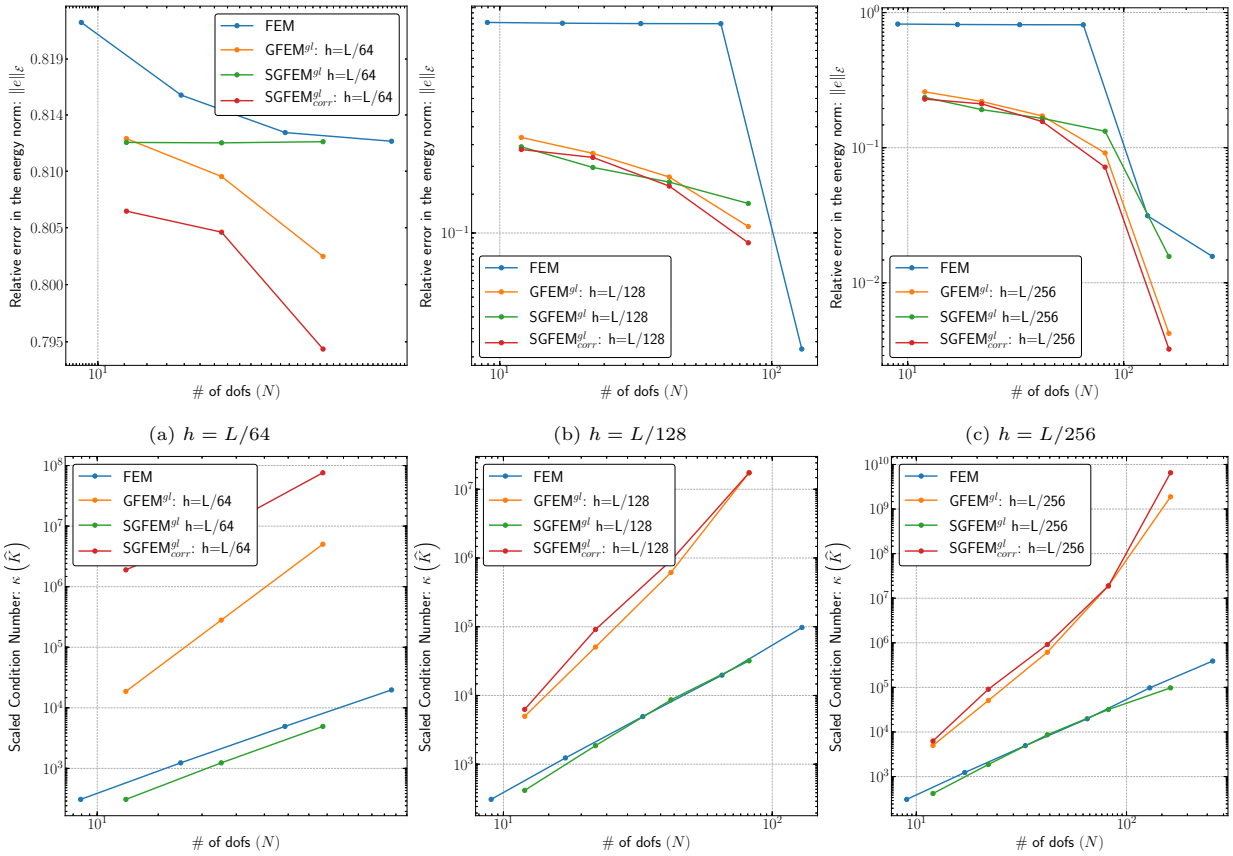

(a) $h = L/64$ (b) $h = L/128$ (c) $h = L/256$

(d) $h = L/64$ (e) $h = L/128$ (f) $h = L/256$

Figure 16: Relative error $\|e\|_{\mathcal{E}}$ and Scaled condition number $\kappa\left(\widehat{K}\right)$ vs No. of dofs (N) for (a) $h = L/64$, (b) $h = L/128$ and (c) $h = L/256$

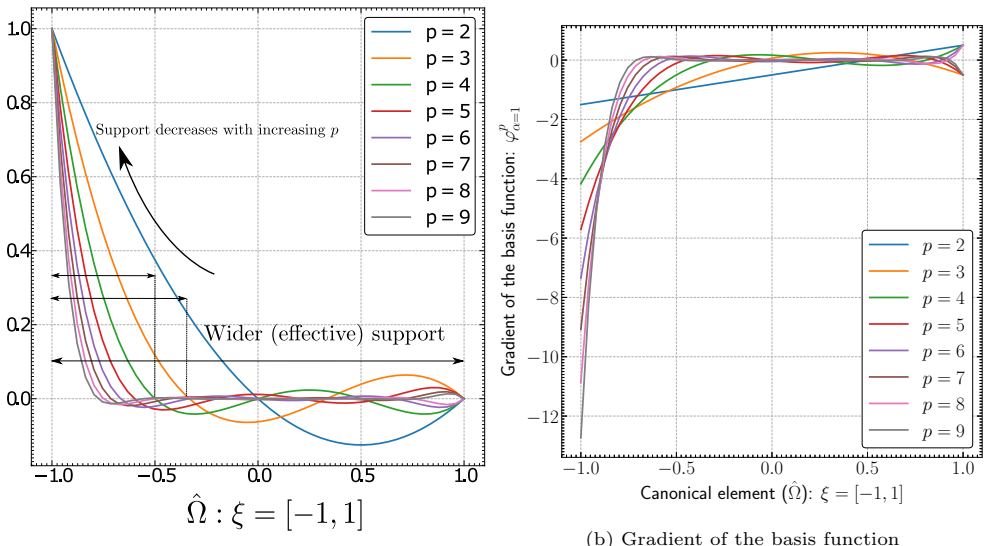

(a) Basis function

(b) Gradient of the basis function

Figure 17: Effective support of the corner basis function in higher order elements

A few remarks regarding the results above:

- The results for SGFEM$^{gl}_{corr}$ are more accurate than corresponding SGFEM^{gl} results. This is due to the absence of the blending element errors in SGFEM$^{gl}_{corr}$. Increasing the order of PoU will reduce this difference further. Physically this can be attributed to the nature of the Lagrange basis functions. As the p order increases the effetive support of first (and the last) basis function in the blending element decreases. Hence the contribution of the GFEM basis to the actual solution decreases in the blending element markedly for higher p. This is illustrated in fig. 17.
- Quadratic and higher order PoU provide an efficient way forward to reduce the blending element errors for GFEM^{gl}, and by the same token SGFEM$^{gl}_{corr}$.

Method	**L/H**	**L/h**	$\|e\|_{\mathcal{E}}$	$\kappa\left(\widehat{K}\right)$
GFEM	8	64	0.812277	1.87E+04
		128	0.260145	4.98E+03
		256	0.258946	4.99E+03
	16	64	0.809074	2.80E+05
		128	0.221799	5.07E+04
		256	0.219863	5.07E+04
	32	64	0.802362	5.03E+06
		128	0.175075	6.15E+05
		256	0.171642	6.15E+05
	64	128	0.106682	1.74E+07
		256	0.091373	1.89E+07
	128	256	4.22E-03	1.88E+09

(a) GFEM^{gl} – Relative Error and Scaled Condition Number

Method	**L/H**	**L/h**	$\|e\|_{\mathcal{E}}$	$\kappa\left(\widehat{K}\right)$
SGFEM	8	64	0.811956	3.08E+02
		128	2.37E-01	4.17E+02
		256	2.36E-01	4.16E+02
	16	64	0.811918	1.23E+03
		128	1.93E-01	1.86E+03
		256	1.91E-01	1.86E+03
	32	64	0.812016	4.94E+03
		128	1.66E-01	8.64E+03
		256	1.65E-01	8.64E+03
	64	128	1.34E-01	3.19E+04
		256	1.32E-01	3.19E+04
	128	256	1.57E-02	9.76E+04

(b) SGFEM^{gl} – Relative Error and Scaled Condition Number

Method	**L/H**	**L/h**	$\|e\|_{\mathcal{E}}$	$\kappa\left(\widehat{K}\right)$
CGFEM	8	64	0.806157	1.89E+06
		128	2.31E-01	6.28E+03
		256	0.228884	6.29E+03
	16	64	0.804392	9.31E+06
		128	2.13E-01	9.10E+04
		256	0.210875	9.07E+04
	32	64	0.794644	7.60E+07
		128	1.60E-01	9.19E+05
		256	0.156072	9.15E+05
	64	128	9.06E-02	1.74E+07
		256	7.17E-02	1.89E+07
	128	256	3.23E-03	6.51E+09

(c) SGFEM$^{gl}_{corr}$ – Relative Error and Scaled Condition Number

Method	**L/H**	**L/h**	$\|e\|_{\mathcal{E}}$	$\kappa\left(\widehat{K}\right)$
FEM	8		0.822182	307.823
	16		0.815976	1233.29
	32		0.812792	4935.17
	64		0.812057	19742.7
	128		0.0313088	97560.8
	256		0.0156856	390245

(d) FEM– Relative Error and Scaled Condition Number

Table 2: BVP2: Summary of the performance of difference enrichment strategies

4. Higher Order FE Calculations

In view of the non-trivial nature of the forcing function in section 3 and the motivation stemming from the rationale presented in fig. 17 a natural choice for FE and corresponding GFEM^{gl} calculations is to use a combination of p-FEM-GFEM^{gl} (but the at expense of higher cost of solving and ill-conditioned matrices). Higher order Lagrange elements enrich the approximation space ($\mathcal{V}_h$) so as to accurately represent functions with smooth derivatives. Therefore the PoU serves to reduce the approximation error as well as the blending element error, whereas GFEM^{gl} helps in approximating the microstructural features.

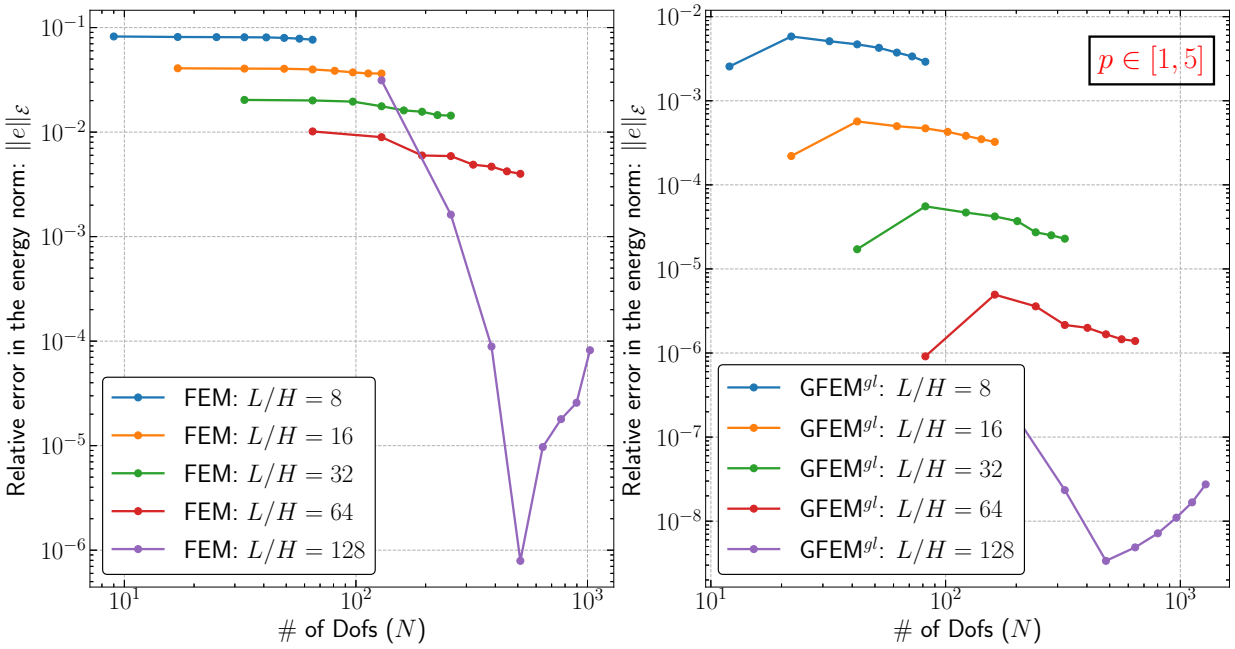

Figure 18: p-FEM-GFEM^{gl} for BVP2

The calculations presented here are computed using both the adaptive quadrature routine `quad` from the `FORTRAN` library `QUADPACK` [4] as well as global Gaussian Quadrature. Also, all the calculations are with respect to conforming local mesh (both $h = L/128$ and $h = L/256$ give nearly the same results). However these are very senstitive to the tolerances due to higher order discontinuous functions (discontinuous gradients in GFEM^{gl} enrichments). Therefore subcell integration with higher order quadrature rules is expected to give more accurate and reliable results for these calculations. Also the error values in the case of GFEM^{gl} particularly those for conforming meshes are near the discretization error, and hence the increase with p order is due to numerical roundoff. The FEM results for the conforming mesh ($H = L/128$) in the above figure on the left show spectral convergence which is characteristic of p-FEM with conforming global mesh. All these results entail the observation in fig. 17 that higher order Lagrange basis functions improve the overall solution in both FEM as well as GFEM^{gl}.

5. Conclusion

GFEM^{gl} was studied for a 1D BVP in elastostatics over a heterogeneous material domain, in presence and absence of a body force by verying both the p-order and the mesh size. Standard FEM requires a fine mesh to capture the fine scale attributes characteristic of composites. GFEM^{gl} performs better than standard FEM for non-conforming meshes. In order to correct the blending element errors, SGFEM$^{gl}_{corr}$ was considered in both section 2 and section 3. Additionally in order to study the conditioning of the linear

systems involved, SGFEM^{gl} was also considered. SGFEM^{gl} offers excellent conditioning properties, and also an added advantage for linear problems without any body force. However SGFEM$^{gl}_{corr}$ performs better in case of problems with body force. As a whole, GFEM^{gl} performs better than competing standard FEM discretization on non-conforming meshes and is therefore a suitable alternative to conforming FEM discretizations for problems with multi-scale features.

References

[1] Ivo Babuška and Uday Banerjee. Stable generalized finite element method (sgfem). *Computer methods in applied mechanics and engineering*, 201:91–111, 2012.

[2] Pavel Bochev and Richard B Lehoucq. On the finite element solution of the pure neumann problem. *SIAM review*, 47(1):50–66, 2005.

[3] Thomas-Peter Fries. A corrected xfem approximation without problems in blending elements. *International Journal for Numerical Methods in Engineering*, 75(5):503–532, 2008.

[4] Robert Piessens, Elise de Doncker-Kapenga, Christoph W Überhuber, and David K Kahaner. *QUADPACK: a subroutine package for automatic integration*, volume 1. Springer Science & Business Media, 2012.

[5] JA Plews and CA Duarte. Bridging multiple structural scales with a generalized finite element method. *International Journal for Numerical Methods in Engineering*, 102(3-4):180–201, 2015.

[6] N. Sukumar, D.L. Chopp, N. Moës, and T. Belytschko. Modeling holes and inclusions by level sets in the extended finite-element method. *Computer Methods in Applied Mechanics and Engineering*, 190(46):6183 – 6200, 2001.

[7] Jinchao Xu and Xiao-Chuan Cai. A preconditioned gmres method for nonsymmetric or indefinite problems. *Mathematics of computation*, 59(200):311–319, 1992.